Obscured Growth of Super Massive Black Holes at the Earliest Universe

Takuma Izumi, [1,2]
[1]*National Astronomical Observatory of Japan, 2–21–1 Osawa, Mitaka, Tokyo 181–8588, Japan*
[2]*Department of Astronomical Science, The Graduate University for Advanced Studies, SOKENDAI, 2–21–1 Osawa, Mitaka, Tokyo*
takuma.izumi@nao.ac.jp

Abstract

I discuss the importance of high resolution and high sensitivity observations of cold molecular gas at the central ~ 100 pc scale region (circumnuclear disk = CND) of a *precursor* of $z > 6-7$ quasars. The usual suspect is a gas-rich starburst galaxy that hosts an obscured active galactic nucleus/AGN (such as an ultra-luminous infrared galaxy = ULIRG). Therefore here I explore a feasibility of 100 pc resolution observations of low-J CO and [C I] emission lines toward a $z = 10$ ULIRG. The planned observations will tell us the CND-scale molecular gas mass, the nature of the obscured heating source (AGN vs starburst), gravitational stability of the CND (potential trigger of mass accretion), and even the black hole mass itself. A synergetic works with future X-ray satellites will also reveal its Eddington ratio. Thanks to the superb capability of ngVLA, we can conduct this ambitious program with a modest investment of the telescope time.

Key words: galaxies: active — galaxies: evolution — galaxies: ISM — galaxies: nuclei

1. Introduction

The discovery of a tight correlation between the masses of central supermassive black holes ($M_{\rm BH}$) and those of galactic bulges ($M_{\rm bulge}$) or the stellar velocity dispersions in the local universe (e.g., Magorrian et al. 1998; Marconi & Hunt 2003; Kormendy & Ho 2013) strongly suggests that the formation and growth of supermassive black holes (SMBHs) and their host galaxies are intimately linked, and the two undergo a co-evolution. Although the detailed mechanism by which the correlation arises is unclear, theoretical models suggest that radiative and kinetic feedback of active galactic nuclei (AGNs) connected to the merger histories of galaxies play a pivotal role (e.g., Di Matteo et al. 2005; Hopkins et al. 2008). Detections of galaxy-scale massive AGN-driven outflows (e.g., Nesvadba et al. 2008; Maiolino et al. 2012; Cicone et al. 2014), likely elevated AGN fraction in interacting/merging galaxies (e.g., Silverman et al. 2011; Goulding et al. 2018), as well as the remarkable similarity of global star formation and SMBH accretion histories (Madau & Dickinson 2014 for a review) would support this evolutionary scheme.

It is intriguing that recent high-resolution simulation works based on the above scheme suggest that even a quasar at z = 7 would show a consistent $M_{\rm BH}$–$M_{\rm bulge}$ relation to the local one, once we properly assess the mass of the host galaxy (Lupi et al. 2019; Marshall et al. 2020). From the observational side, $z > 6$ quasar host galaxies have been extensively studied at long-wavelength (e.g., submm) as these galaxies are hard to detect at rest-frame UV to optical due to the outshining brightness of the nuclei (Mechtley et al 2012). Previous high resolution [C II] emission line observations, mainly performed by using the Atacama Large Millimeter/submillimeter Array (ALMA), provided basic star-forming nature and dynamical mass ($M_{\rm dyn}$) of those host galaxies (e.g., Wang et al. 2013; Venemans et al. 2016). These works revealed that $z > 6$ quasars are typically hosted by vigorous starburst galaxies (star-formation rate SFR $\gtrsim 100-1000\ M_\odot\ {\rm yr}^{-1}$), and have *over-massive* supermassive black holes (SMBHs) relative to the local co-evolution relation (i.e., their $M_{\rm BH}$ is $\sim 10\times$ more massive than what is expected from the local relation)[1]. However, previous observations would be highly biased toward the most luminous quasars (1450Å magnitude $M_{1450} < -26$), which correspond to the most massive SMBH population that accordingly bias the observed shape of the $z > 6$ co-evolution relation (Lauer et al. 2007).

Recent ALMA observations toward $z \sim 6-7$ optically *low-luminosity* quasars ($M_{1450} > -25$), that typically have lower mass $M_{\rm BH}$ than the luminous ones, however, have started to show that these low-luminosity (= less-biased) objects tend to follow the local co-evolution relation (Izumi et al. 2018, 2019): this is consistent with the hydrodynamic model predictions indeed (Marshall et al. 2020). It is noteworthy that such low-luminosity quasars are nowadays, and will be, routinely discovered from wide area and deep optical imaging surveys by using, e.g., Subaru Hyper Suprime-Cam (HSC) and Vera C. Rubin Observatory (VRO). With this momentum, we will sooner or later be able to obtain a census of star-forming and dynamical nature of *quasars* even at $z \sim 6-7$.

2. Hunt for a dusty precursor

The emergence of the quasars, as well as the co-evolution relation already at $z \sim 6-7$, require a quite rapid process for the early galaxy/SMBH formation and evolution. The *usual suspect* is mergers of gas-rich galaxies, which can drive a growth of massive galaxies and SMBHs with a reasonably short timescale of $\lesssim 1$ Gyr (e.g., Hopkins et al. 2008). Such a merger-induced active galaxy appears as a dusty starburst known as an ultra-luminous infrared galaxy (ULIRG) in the local uni-

[1] We need to equate $M_{\rm dyn}$ to $M_{\rm bulge}$ as we do not have any information on their host galaxy stellar light until the operation of the James Webb Space Telescope.

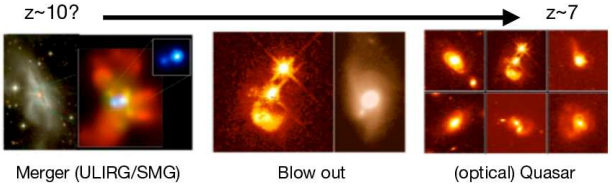

Fig. 1. An expected evolutionary sequence from a gas-rich merger to an optical quasar (figure modified from Hopkins et al. 2008). Given the already known existence of quasars at $z \sim 7.5$, we will try to characterize their precursors at further higher redshifts such as $z \sim 10$.

Table 1. Target Emission Lines

Transition	$\nu_{\rm rest}$ (GHz)	$E_u/k_{\rm B}$ (K)	$n_{\rm cr}$ (cm^{-3})
CO(1–0)	115.271	5.5	2.1×10^3
CO(2–1)	230.538	16.6	1.1×10^4
CO(3–2)	345.796	33.2	3.6×10^4
[C I](1–0)	492.161	23.6	1.2×10^3
[C I](2–1)	809.342	62.5	3.1×10^3

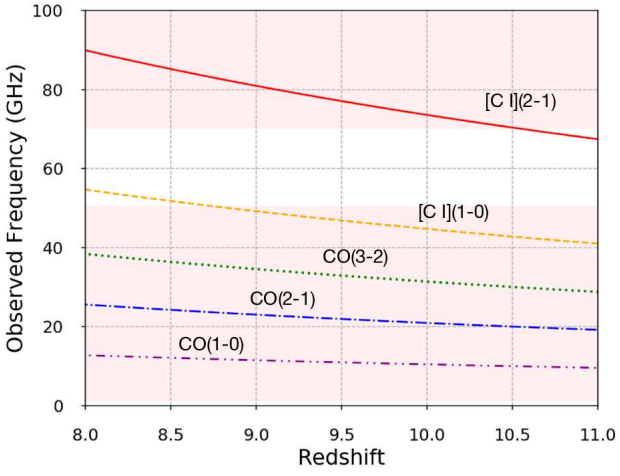

Fig. 2. Observed frequencies of our target emission lines (^{12}CO and [C I]) as a function of redshift. Shaded regions indicate the frequency coverage of ngVLA. As shown here, we can observe all these lines from galaxies at $z \sim 10$, for example.

verse and/or a submillimeter galaxy (SMG) at higher redshifts. Therefore, it is intriguing to uncover such ULIRG/SMG-class galaxies at a significantly earlier universe than $z \sim 7.5$ (current redshift-record of quasars, Wang et al. 2021), e.g., $z \sim 10$ (Figure 1), and characterize their properties.

However, such starburst galaxies at $z > 7$ must be quite rare: a recent observational estimate on IR luminosity function at $4.5 < z < 6$ shows a number density of ULIRG-class objects ($10^{12} < L_{\rm IR}/L_\odot < 10^{13}$) is as low as $\lesssim 10^{-4}$ Mpc^{-3} dex^{-1} (Gruppioni et al. 2020). We thus need to perform an ultra-wide area and deep survey at first to identify such objects. Next generation 50 m-class single dish telescopes that have $\sim$ deg^2 field-of-view (e.g., Large Submillimeter Telescope = LST) will be able to conduct deep spectroscopic surveys over a wide area on the sky, with the aid of ultra-wide bandwidth superconducting spectrometers (Endo et al. 2019).

3. Extensive characterization with ngVLA

I hereafter discuss possible follow-up observations for those newly detected starburst systems at $z > 7.5$, with mainly focusing on a $z = 10$ object ($1'' = 4.2$ kpc) as an educational example (Figure 1). Suppose firstly that there is a hidden AGN at its nucleus behind the curtain of dust, which would be experiencing a rapid mass accretion given the blessed availability of gas. As explained later, we will attempt to measure a cold molecular gas mass ($M_{\rm mol}$) of the system. Hence our target emission lines (Table 1) may include the low-J ^{12}CO lines (classical proxies of $M_{\rm mol}$; Bolatto et al. 2013), and atomic carbon fine structure lines ([C I]) that are nowadays considered to be another good proxies of $M_{\rm mol}$ in various environments, particularly in high-redshift galaxies (e.g., Papadopoulos & Greve 2004; Israel et al. 2015; Jiao et al. 2017; Valentino et al. 2018): these emission lines of a $z \gtrsim 8$ galaxy fall well into the frequency coverage of the next generation Very Large Array (ngVLA, Figure 2).

Thanks to the extremely high angular resolution and sensitivity provided by ngVLA, we can investigate the following key topics regarding the *obscured AGN*.

(1) How massive is a circumnuclear gas disk? A number of theoretical works and local observations claim an importance of sub-kpc-scale circumnuclear gas disk (CND) formed around an AGN as a direct reservoir of fuel onto the SMBH (e.g., Thompson et al. 2005; Kawakatu & Wada 2008; Izumi et al. 2016). A key physical process here to drive gas inflows would be a gravitational instability of the disk (Toomre 1964). We will assess this by measuring the gas mass and dynamical properties of the CND. The low-J CO lines and the [C I] lines can be used to measure $M_{\rm mol}$, if we have *proper conversion factors* from the line luminosity to $M_{\rm mol}$ for AGN environments. We should really care about this point as AGN can alter the chemical composition of the surrounding gas (see the item-(2) in the following), which would make the conversion factors significantly different from what measured for systems without AGN (e.g., Bolatto et al. 2013; Jiao et al. 2017).

Such proper conversion factors can be estimated from extensive analyses of high resolution line emission data and stellar mass distribution data of nearby active galaxies. For example, Izumi et al. (2020) modeled the CO(2–1) and the [C I](1–0) velocity fields of the type-1 Seyfert galaxy NGC 7469 to obtain radial profiles of dynamical mass ($M_{\rm dyn}$). They subtracted a stellar mass distribution measured by using the Hubble Space Telescope from this $M_{\rm dyn}$ to directly obtain $M_{\rm mol}$ radial distribution as a residual. This procedure directly provides the conversion factors after dividing the $M_{\rm mol}$ by $L'_{\rm CO}$ or $L'_{\rm [CI]}$. Systematic applications of this method to nearby AGNs by using ALMA, for example, will deliver the conversion factors in a statistical manner: we can therefore apply them to high redshift objects in the ngVLA era.

(2) How to show the existence of an obscured AGN? Almost by definition, it is virtually impossible in an ULIRG-class object to detect the light directly emerging from the AGN at rest-frame UV-to-optical wavelengths due to severe dust-extinction (i.e., difficult to reveal the existence of an obscured

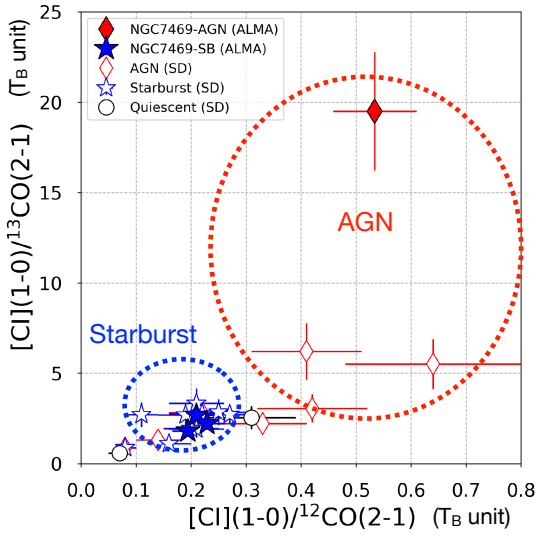

Fig. 3. [C I](1–0)/^{12}CO(2–1) vs [C I](1–0)/^{13}CO(2–1) line flux ratios ($T_{\rm B}$ unit) of various nearby galaxies (figure modified from Izumi et al. 2020). High resolution ($\sim$ 130 pc) ALMA observations toward the CND and the surrounding starburst region of NGC 7469 (nearby type-1 AGN) are shown by the filled symbols. The open symbols indicate the literature data taken by single dish (SD) telescopes, color-coded as a function of their nuclear types (AGN, starburst, quiescent). One can see that the line ratios are elevated in AGN systems, particularly when observed at a high-resolution that selectively probes the CND (XDR).

AGN). However, we will overcome this issue with the combination of the target emission lines. We emphasize that one very unique point of AGNs, as compared to star-formation, is that AGNs are a powerful source of hard X-ray radiation in the universe. Hence X-ray dominated regions (XDRs, Maloney et al. 1996; Meijerink and Spaans 2005), where gas physical and chemical properties are governed by the X-ray radiation, should form around them. It is striking in this context that Izumi et al. (2020) found a markedly elevated [C I](1–0)/CO(2–1) and/or [C I](1–0)/^{13}CO(2–1) line ratios at the $\sim$ 100 pc-scale CND of NGC 7469 as compared to starburst regions of the same galaxy, as well as to local starburst galaxies (Figure 2). According to non-LTE calculation, they concluded that this enhancement is due to an elevated C abundance relative to CO, which is a natural consequence in an XDR as CO is efficiently dissociated there. With the superb angular resolution of ngVLA, we can properly map the central $\sim$ 100 pc regions even in $z \sim 10$ galaxies at which we expect to see XDR signatures (Schleicher et al. 2010), and capture this chemically-driven line enhancement as an *extinction-free indicator of AGN*.

(3) What is the characteristic feature of that AGN? Synergies with future projects. If an obscured AGN indeed corresponds to an early evolutionary phase of cosmic SMBH growth as expected in the merger-induced evolutionary models (e.g., Hopkins et al. 2008), that AGN would have a smaller $M_{\rm BH}$ and a higher Eddington ratio (probably a *Super-Eddington* ratio) than previously-identified normal optical quasars at $z \sim 6-7$ ($M_{\rm BH} \sim 10^9\ M_\odot$, Eddington ratio $\sim$0.1 – 1, e.g., Onoue et al. 2019). We will try to measure these basic properties of obscured AGNs at $z \sim 10$ with ngVLA.

Recent high resolution ALMA observations of CO lines in the local universe have demonstrated the great power of cold gas dynamics measurement to constrain $M_{\rm BH}$ by capturing the Keplerian steep rise in a rotation curve (e.g., Davis 2014; Onishi et al. 2015; Nguyen et al. 2020). We may naturally apply this methodology to higher redshift objects with ngVLA. However, as most of the previous cold gas works on $M_{\rm BH}$ measurement were conducted toward relatively quiescent galaxies, one caveat would be again the XDR effect on the gas composition (CO dissociation). We can overcome this issue by focusing on the [C I] lines instead, as shown in Figure 4, which is the case of NGC 7469, a luminous AGN in the nearby universe. One can clearly see that the [C I](1–0) line is more centrally concentrated than CO(1–0), which is a natural consequence of the XDR effect. Therefore, even if the XDR effect matters in obscured AGNs at $z \sim 10$, we will still be able to constrain their $M_{\rm BH}$ by observing [C I] lines. Note that we do need stellar mass distribution data to better model the gravitational potential of the galaxy. This will become feasible once next generation large optical/NIR telescopes (e.g., European Extremely Large Telescope = E-ELT, Thirty-Meter Telescope = TMT) start to operate.

Synergies with future X-ray satellites will be of our interest as well. The ESA's Athena satellite and the NASA's Lynx satellite planned in 2030s will efficiently sample the rest-frame >10 keV photons with extremely high sensitivities that will reach $z \sim 10$ universe. This high-energy range does not significantly suffer from the Compton thickness effect, hence probes the intrinsic AGN luminosity in a least biased manner. Combined with $M_{\rm BH}$ estimated by ngVLA, we will be able to assess the Eddington ratio even for an obscured object at that high redshift.

4. Feasibility?

In order to dynamically measure the $M_{\rm BH}$, as well as to selectively probe the XDR-like spatial scales, we here suppose to perform a 100 pc (0$''$.024) resolution CO and [C I] emission line observations toward a $z = 10$ galaxy (with an obscured AGN). Note that this resolution is still worse than the typical sphere of influence (SOI) size of a $10^8\ M_\odot$ SMBH (several $\times$10 pc), but the SOI criterion does not necessarily apply for cold gas dynamics-based $M_{\rm BH}$ measurements as shown in previous works (Davis 2014; Nguyen et al. 2020).

Suppose that there is $4 \times 10^9\ M_\odot$ molecular gas within this 100 pc aperture, which is roughly the case of the nearby ULIRG Arp 220 (Scoville et al. 2015). If we apply the CO(1–0)-to- and [C I](1–0)-to-molecular mass conversion factors derived at the XDR scale of NGC 7469 (Izumi et al. 2020), namely $\alpha_{\rm CO} = 4.1$ and $\alpha_{\rm CI} = 4.4\ M_\odot$ (K km s^{-1} pc^2)$^{-1}$, we obtain corresponding velocity-integrated line fluxes of $S\Delta V_{\rm CO10} = 4.1 \times 10^{-4}$ (at $\nu_{\rm obs} = 10.5$ GHz) and $S\Delta V_{\rm [CI]10} = 6.9 \times 10^{-3}$ Jy km s^{-1} (at $\nu_{\rm obs} = 44.7$ GHz), respectively ($z = 10$). By assuming a CO(2–1)/CO(1–0) ratio of $\sim$ 7 measured at the central $\sim$ 100 pc of NGC 7469 (Izumi et al. 2020), as well as a [C I](2–1)/[C I](1–0) of $\sim$ 2 found in the galaxy-wide scale of ULIRG-class objects (Jiao et al. 2017) [2], we

[2] Currently we do not have a good measurement of this ratio at the central

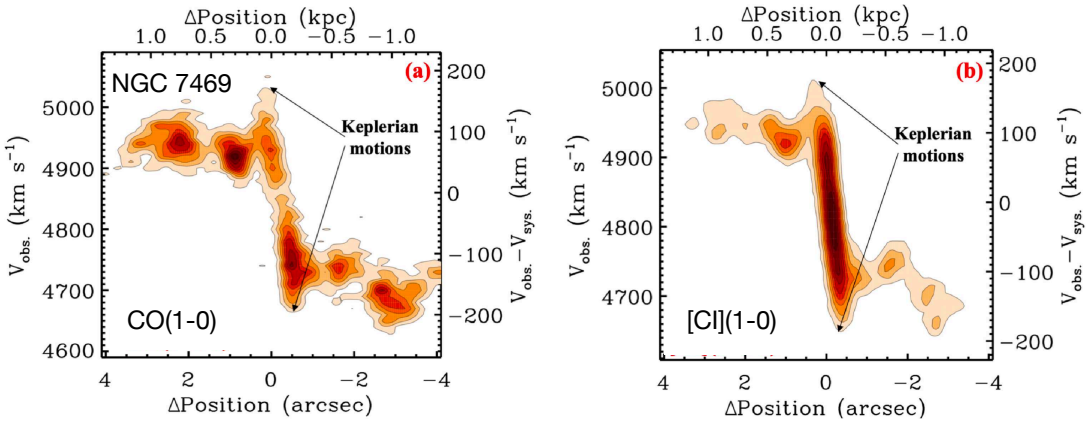

Fig. 4. Position-velocity diagrams of (a) CO(1–0) and (b) [C I](1–0) cut along the kinematic major axis of NGC 7469, a luminous type-1 AGN (figure adopted from Nguyen et al. 2021). One can clearly see that [C I](1–0) is more concentrated toward the center (AGN) than CO(1–0), which is a clear consequence of the XDR effect (CO dissociation).

then obtain $S\Delta V_{\rm CO21} = 2.8 \times 10^{-3}$ (at $\nu_{\rm obs} = 21.0$ GHz) and $S\Delta V_{\rm [CI]21} = 1.4 \times 10^{-2}$ Jy km s^{-1} (at $\nu_{\rm obs} = 73.6$ GHz). Although it is highly dependent on the adopted conversion factors, the potentially brighter line flux of [C I](2–1) suggests that it would be more prioritized than CO(2–1) to probe the gas dynamics. However, CO(2–1) can still be used to take a line ratio to diagnose the hidden energy source of the system (Figure 3).

If we further assume a Gaussian line profile (FWHM = 300 km s^{-1}) for both CO(2–1) and [C I](2–1), we will obtain

- CO(2–1): S/N ~ 5 at the Gaussian profile peak, with an on-source time of 25 hr and a velocity resolution of $dV = 100$ km s^{-1},
- [C I](2–1): S/N ~ 15 at the Gaussian profile peak, with an on-source time of 30 hr and $dV = 50$ km s^{-1},

according to the ngVLA key performance matrix. The S/N of the [C I](2–1) observation will be fine to perform dynamical modelings of the observed velocity field. Although this is still a significant investment of the telescope time for a single object, I would claim it is worth conducting given the obvious extreme rarity of $z = 10$ ULIRG-like galaxies.

One would care about the additional heating effect and the brightness contrast effect due to the high temperature (30 K at $z = 10$) cosmic microwave background (CMB) radiation (da Cunha et al. 2013). This is indeed a nightmare for normal star-forming and/or quiescent galaxy observations. However, now that we focus on a very active galaxy, we would naively expect both the gas density and the kinetic temperature are high, i.e., gas excitation is reasonably high. Therefore, if the line excitation temperature of these lines exceeds 100 K, for example, we can recover $\gtrsim 75\%$ and $\gtrsim 80\%$ of the intrinsic line fluxes of CO(2–1) and [C I](2–1) against the CMB, respectively, which do not significantly affect the detectability of these lines.

100 pc-scale of external galaxies. Near-future ALMA observations will constrain this. We thus keep using the galaxy-scale (>kpc-scale) measurement in this document.

5. Summary

Given the existence of quasars at $z > 6-7$, as well as the rapid emergence of the co-evolution relation already at $z \sim 6-7$ (e.g., Izumi et al. 2018, 2019), it is urgent to identify and characterize their precursors at further higher redshifts. Possible candidates include a dusty ULIRG-like galaxy formed by a major merger of gas-rich galaxies, which will be uncovered by future wide-area single dish spectroscopic/imaging surveys. In this document, I briefly discuss high resolution (100 pc) CO and [C I] observations toward such a dusty galaxy at $z = 10$ that harbors an obscured AGN. Thanks to the superb capability of ngVLA, we will be able to diagnose the obscured heating source (AGN vs starburst), to measure the CND-scale molecular gas mass, to assess the gravitational stability of that disk (a likely key physical process to trigger inflows), and to estimate the SMBH mass. We can further constrain the Eddington ratio of that SMBH as a synergy with future X-ray satellites. Therefore, ngVLA has a great capability to explore the obscured phase of SMBH growth even at that earliest universe.

References

Bolatto, A. D., Wolfire, M., & Leroy, A. K. 2013, ARA&A, 51, 207
Cicone, C., et al. 2014, A&A, 562, A21
da Cunha, E., et al. 2013, ApJ, 766, 13
Davis, T. A. 2014, MNRAS, 443, 911
Di Matteo, T., Springel, V., & Hernquist, L. 2005, Nature, 433, 604
Endo, A., et al. 2019, Nature Astronomy, 3, 989
Goulding, A. D., et al. 2018, PASJ, 70, S37
Gruppioni, C., et al. 2020, A&A, 643, A8
Hopkins, P. F., et al. 2008, ApJS, 175, 356
Israel, F. P., Rosenberg, M. J. F., & van der Werf, P. 2015, A&A, 578, A95
Izumi, T., Kawakatu, N., & Kohno, K. 2016, ApJ, 827, 81
Izumi, T., et al. 2018, PASJ, 70, 36
Izumi, T., et al. 2019, PASJ, 71, 111
Izumi, T., et al. 2020, ApJ, 898, 75
Jiao, Q., et al. 2017, ApJL, 840, L18
Kawakatu, N., & Wada, K. 2008, ApJ, 681, 73

Kormendy, J., Ho, L. C. 2013, ARA&A, 51, 511
Lauer, T. R., et al. 2007, ApJ, 670, 249
Lupi, A., et al. 2019, MNRAS, 488, 4004
Madau, P., & Dickinson, M. 2014, ARA&A, 52, 415
Magorrian, J., et al. 1998, AJ, 115, 2285
Maiolino, R., et al. 2012, MNRAS, 425, L66
Maloney, P. R., Hollenbach, D. J., & Tielens, A. G. G. M. 1996, ApJ, 466, 561
Marconi, A., & Hunt, L. K. 2003, ApJL, 589, L21
Marshall, M. A., et al. 2020, MNRAS, 499, 3819
Mechtley, M., et al. 2012, ApJL, 756, L38
Meijerink, R., & Spaans, M. 2005, A&A, 436, 397
Nesvadba, N. P. H., et al. 2008, A&A, 491, 407
Nguyen, D. D., et al. 2020, ApJ, 892, 68
Nguyen, D. D., et al. 2021, submitted to MNRAS
Onishi, K., et al. 2015, ApJ, 806, 39
Onoue, M., et al. 2019, ApJ, 880, 77
Papadopoulos, P. P., & Greve, T. R. 2004, ApJL, 615, L29
Schleicher, D. R. G., Spaans, M., & Klessen, R. S. 2010, A&A, 513, A7
Scoville, N., et al. 2015, ApJ, 800, 70
Silverman, J. D., et al. 2011, ApJ, 743, 2
Thompson, T. A., Quataert, E., & Murray, N. 2005, ApJ, 630, 167
Toomre, A. 1964, ApJ, 139, 1217
Valentino, F., et al. 2018, ApJ, 869, 27
Venemans, B. P., et al. 2016, ApJ, 816, 37
Wang, F., et al. 2021, ApJL, 907, 1
Wang, R., et al. 2013, ApJ, 773, 44